Edible oil-in-water emulsions prepared using viscoelastic solutions of a sucrose ester

Xin Hu,[1,2] Bernard P. Binks,[2,*] Zhenggang Cui[1,*]

[1] *The Key Laboratory of Synthetic and Biological Colloids, Ministry of Education, School of Chemical and Material Engineering, Jiangnan University, Wuxi, China*

[2] *Department of Chemistry, University of Hull, Hull. HU6 7RX. UK*

Submitted to: Colloids & Surfaces A on ? March, 2022

Contains ESI

*Corresponding authors: b.p.binks@hull.ac.uk; cuizhenggang@hotmail.com

Abstract

Sucrose esters which are non-toxic and biodegradable nonionic surfactants have been widely applied as food emulsifiers. Generally, hydrophilic and hydrophobic sucrose esters are good oil-in-water and water-in-oil emulsifiers respectively, but the sucrose esters of intermediate HLB values (6-8) are not good emulsifiers. In this work, the emulsification properties of sucrose stearate C-1807 with HLB = 7 with edible oils were examined for canola oil, olive oil and soybean oil. It is found that C-1807 forms multilamellar vesicles in aqueous solution at concentrations beyond 5.2×10^{-4} wt.%. Although monomeric C-1807 is not a good emulsifier, the vesicles can significantly improve the stability of edible oil-in-water emulsions with ϕ_o = 0.5. When the concentration of surfactant is increased to 2 wt.%, the aqueous phase becomes viscoelastic and shows gel-like behavior, by which high internal phase emulsions (HIPEs) with ϕ_o = 0.75 can be formed for the three edible oils. Although the HIPEs are not stable against harsh freeze-thaw cycles between -20 °C and 30 °C, they are stable against cooling-heating cycles between 5 °C and 30 °C. The viscoelastic aqueous phase provides gel-like strength and the vesicles dispersed in the aqueous lamellae surrounding oil droplets prevent them from flocculation and coalescence. This provides a protocol for sucrose esters like C-1807 to be used as food-grade emulsifier in emulsion products.

Keywords: Sucrose stearate, Vesicles, Viscoelasticity solution, High internal phase emulsions, Cooling-heating

Introduction

Sucrose esters are amphiphilic nonionic surfactants composed of an uncharged hydrophilic sucrose ring and long chain hydrocarbon lipophilic groups. Thanks to the non-toxicity, high biodegradability, good taste and aroma profile in comparison with petrochemically derived products, sucrose esters have been widely applied in food, cosmetic and pharmaceutical industries.[1-5] Moreover, they are derived from renewable sucrose and vegetable oils and are therefore environmentally friendly products.[6] Some sucrose esters have a Drug Master File what is this? (Drug Master File means files of drug administration), and sucrose stearates and sucrose palmitates have been featured in European Pharmacopoeia and in United States Pharmacopeia/National Formulary confirming their human applicability.[4] Therefore, there has been growing interest with sucrose esters.

Generally, surfactants can self-assemble into different aggregates in aqueous solution, such as micelles[7] and vesicles,[8] depending on their molecular structure and solution conditions, *e.g.* pH, temperature, presence of additives. Accordingly, hydrophobic surfactants may form reversed micelles and reversed vesicles in oil media.[9-11] Most sucrose esters have been reported to form either vesicles or reversed vesicles. For example, Ishigaml and Machlda[12] observed vesicles of 70-700 nm formed by sucrose dilaurate using transmission electron microscopy. Valdés *et al.*[4] prepared vesicles using two commercial sucrose ester products, S-570 and S-770, containing both monoesters and diesters respectively, and investigated their properties such as size, zeta potential and effects of pH. Also, the formation of reversed vesicles of sucrose esters in silicone oil, mixed silicone oils as well as isopropyl palmitate has also been studied.[13] These normal vesicles and reversed vesicles formed by nonionic surfactants are significant for drug delivery systems.[4,14-16]

It is also known that surfactants may form viscoelastic solutions by aggregating into either entangled wormlike micelles or densely packed multi- or unilamellar vesicles.[17] Some researches have focused on the viscoelastic characteristics of solutions of wormlike micelles,[18-20] as they are three-dimensionally intertwined. For example, Hu

et al.[19] used ionic liquid-type surfactant [$C_{16}imC_8$] to prepare viscoelastic wormlike micelles and synthesize CdS quantum dots with different additives. Shibaev *et al.*[20] studied the phase behavior and rheological properties of mixed wormlike micelle solutions of a cationic surfactant, erucyl-bis(hydroxyethyl) methyl ammonium chloride, and oppositely charged polyelectrolyte xanthan. The viscoelastic wormlike micelle systems have been applied as size-controllable microreactors for aqueous chemical reactions[21] and as templates for materials synthesis.[22] It has been reported that the rheological properties and phase behavior of the densely packed vesicle solutions look very like that of wormlike micelle solutions, and both systems can be shear thinning and the storage modulus can be an order of magnitude larger than the loss modulus.[17] Although the characteristics of vesicle gels have been involved in many investigations,[23-25] the characteristics of vesicle solutions are rarely reported.

Oil-in-water emulsions have been widely applied in food, cosmetic and pharmaceutical products in which high internal phase emulsions (HIPEs) having an internal phase volume fraction beyond the close packing limit (> 0.74) are especially important due to their special characteristics.[26-30] The HIPEs are semi-solid materials showing viscoelastic character,[27] which may impact the spreadability of foods or cosmetics.[28] The droplets in HIPEs normally have polyhedron shapes due to their close proximity.[29] HIPEs have potential to enhance the viability of probiotics during food processing and storage[31] and to encapsulate nutraceuticals like β-carotene,[28,32] curcumin[33] and algal oils[34,35] for enhancing solubility, bioavailability and chemical stability of these substances. In addition, HIPEs can also be used as substitute for saturated fatty acids and hydrogenated oils[36] and as templates for creating porous materials with well-defined pore characteristics.[37] Nevertheless it is worth noting that conventional HIPEs are commonly stabilized against coalescence using high concentrations of surfactant ($\geqslant$ 5%)[38] and the studies on the cooling-heating and freeze-thaw stability of these HIPEs are rarely reported.

In this work, we report on the properties of aqueous solutions of sucrose stearate C-1807, which has an intermediate HLB number of 7 and can form vesicles at

concentrations beyond the critical aggregate concentration (CAC). At relatively high C-1807 concentration, the vesicle solution becomes viscoelastic and edible oil-in-water emulsions including HIPEs can be prepared with several edible oils (canola oil, soybean oil and olive oil) of different melting point. The stabilization of the emulsions at different C-1807 concentrations and especially the cooling-heating and freeze-thaw stability of the HIPEs were examined. It is found that although monomeric C-1807 is not a good emulsifier, the viscoelastic solutions obtained at relatively high concentration (2 wt.%) can significantly improve the stability of emulsions including HIPEs. The formation of vesicles beyond the CAC and the gel-like strength of the viscoelastic solutions are responsible for the stabilization. In addition, the edible oil-in-water emulsions formed display excellent stability in cooling-heating cycles between 5 and 30 °C although they are less stable after freeze-thaw cycles between -20 and 30 °C.

Experimental

Materials

Sucrose stearate (tradename C-1807, food/cosmetic-grade, with 40 wt.% monoester and 60% di-/tri-/polyesters, HLB = 7 quoted by the supplier) was provided as a white powder by Mitsubishi-Kagaku Foods Corporation (Tokyo). Canola oil and soybean oil were purchased from a local store (Wuxi, China) and the olive oil was from Macklin Company (China) all with food-grade specifications. The fatty acid compositions were measured by gas chromatography-mass spectrometry (GC/MS) in the form of methyl esters (FAMEs) as shown in Table S1. Water was treated with a Milli-Q reagent system until a resistivity of 18 MΩ cm was reached.

Preparation and characterization of aqueous C-1807 solutions

A stock aqueous dispersion of C-1807 at a concentration of 2 wt.% was prepared using pure water, which was placed in a water bath of 60 ℃ until all the surfactant dissolved and then left to cool to room temperature (25 ℃).[39] The stock dispersion was then diluted to different concentrations, with those at low concentration being

transparent solutions. The surface tension of aqueous C-1807 solutions/dispersions was determined using du Noüy ring method at 25 ± 0.5 ℃. Before measurement, all samples (20 mL in measuring cell) were stored in an incubator at 25.0 ± 0.5 ℃ for more than 48 h. The platinum-iridium ring was rinsed with ethanol followed by heating to glowing in a flame prior to measurement.

Dynamic light scattering (DLS) was used to determine the average diameter of the aggregates present in aqueous dispersions. Measurements were carried out at 25 ℃ with a Zetasizer Nano ZS (Malvern Instruments) equipped with a 4 mW He-Ne laser beam operating at λ = 633 nm under a scattering angle of 173°. The aqueous dispersions of C-1807 at different concentrations were poured into polystyrene cuvettes (U-shape), and three measurements were conducted for each sample. The zeta potential of the C-1807 dispersions at different concentrations was measured at 25 ℃ by the same instrument with the Smoluchowski approximation being used to convert measured electrophoretic mobilities to zeta potential, and the result is the average of at least three measurements.

The samples for cryogenic Transmission Electron Microscopy (cryo-TEM) observation were prepared in a controlled-environment vitrification system (CEVS). A micropipette was used to load 1 μL of aqueous dispersion (what is this? “hydrogel” is changed to aqueous dispersion) onto a TEM copper grid, which was blotted with two pieces of filter paper resulting in a thin film suspended on the mesh. The grid was then quickly plunged into a reservoir of liquid ethane (cooled by nitrogen) at -165 °C. The vitrified samples were then stored in liquid nitrogen until they were transferred into a cryogenic sample holder (Gatan 655) and examined using a Talos F200C (200 kV) at approximately -174 °C. The images were recorded on a Gatan multiscan CCD and processed using Digital Micrograph.

Rheological measurements were performed on a stress-controlled rheometer (Discovery DHR-3, TA Instruments) with a cone-plate sensor at 25 °C. The cone was composed of standard ETC steel with a diameter of 40 mm and a cone angle of 2°. The gap between the centre of the cone and the plate was 53 μm. Before the test, a stress

sweep was performed at a frequency of 1.0 Hz. A stress value was then chosen to ensure that the sample was in the linear viscoelastic region during the subsequent oscillatory measurements. The samples were measured at 25 °C throughout the experiments. Each regained gel sample was kept on the plate for 5 min to reach equilibrium before testing.

Preparation and characterization of emulsions

Equal volumes (5 mL) of aqueous C-1807 dispersion and an edible oil were added to a screw-top glass vial (i.d. = 1.6 cm, height = 7.2 cm). The two phases were emulsified using an IKA Ultra Turrax T 25 homogenizer with a 1 cm head operating at 11,000 rpm for 2 min. All the experiments were conducted at room temperature (~25 °C) unless stated otherwise. Photos of the vessels were taken just after preparation and at subsequent times to evaluate the emulsion stability. The emulsion type was inferred from the drop test. If emulsion drops disperse in water but sediment in oil, it indicates an oil-in-water (O/W) emulsion and *vice versa*. The stability of O/W emulsions to creaming was assessed by monitoring the position of the water-emulsion interface, and the stability to coalescence was measured by following the change in the height of the clear oil-emulsion interface. Creaming is represented by the fraction of water (f_w) released:

$$f_w = V_{w(t)}/V_{w(0)} \quad (1)$$

where $V_{w(t)}$ is the volume of water extracted at t min and $V_{w(0)}$ is the initial water volume before homogenization. Similarly, coalescence is represented by f_o:

$$f_o = V_{o(t)} / V_{o(0)} \quad (2)$$

where $V_{o(t)}$ is the volume of oil extracted at t min and $V_{o(0)}$ is the initial oil volume before homogenization.

The preparation of HIPEs was similar, in which the total volume of the emulsion was kept at 10 mL with the volume of oil ≥ 7.5 mL. Micrographs of the prepared emulsions were taken using a VMX40M microscope and VistarImage software. The emulsion (30 μL) was diluted with the corresponding aqueous phase (30 μL) on a glass slide (Thermo Scientific) and then observed under the microscope. Rheological

measurements of emulsions were carried out similar as for C-1807 aqueous solutions described above.

Cooling-heating and freeze-thaw stability of emulsions

To test the cooling-heating and freeze-thaw stability of an emulsion, the emulsions were stored in a thermostat bath or a freezer at 5 ℃ and -20 ℃ respectively, for 22 h and then heated or thawed to 30 ℃ for 2 h (one cycle). Every sample experienced three cooling-heating or freeze-thaw cycles and the experiment was done in triplicate. The thermal behaviour of emulsions was characterized using differential scanning calorimetry (DSC) using a Netzsch DSC 204 F1 (Germany) with Netzsch-Proteus-61 software. Nitrogen was used as the purge gas and the calibration was done with a sample of indium. The sample (~10 mg) was placed in a 40 μL aluminium pan sealed by a lid, and was then cooled from 30 °C to -30 °C at a rate of 5 °C/min and then re-heated to 30 °C at the same rate. For each sample, the cooling and heating cycle was repeated three times.

Results and discussion

(a) Characterization of aqueous C-1807 dispersions

A series of C-1807 aqueous dispersions at different concentrations was prepared and their surface tension was measured. The appearance of these dispersions at 25 ℃ is shown in Figure 1(a), where they change from transparent solutions to turbid dispersions with increasing concentration. The surface tension of the solutions is shown in Figure 1(b) which decreases with increasing concentration and approaches a plateau value beyond a critical aggregation concentration (CAC);[40] the surface tension at the CAC is denoted as γ_{CAC}. The break point in Figure 1(b) gives a CAC of 5.4×10^{-4} wt.% and γ_{CAC} of 47.6 mN/m in water at 25 °C. Compared with the photos in Figure 1(a) it is noticed that just beyond the break point the solutions are transparent, suggesting formation of aggregates of small size near the CAC. However, the dispersions at higher concentrations (> 0.1 wt.%) become turbid suggesting formation of larger sized

aggregates.

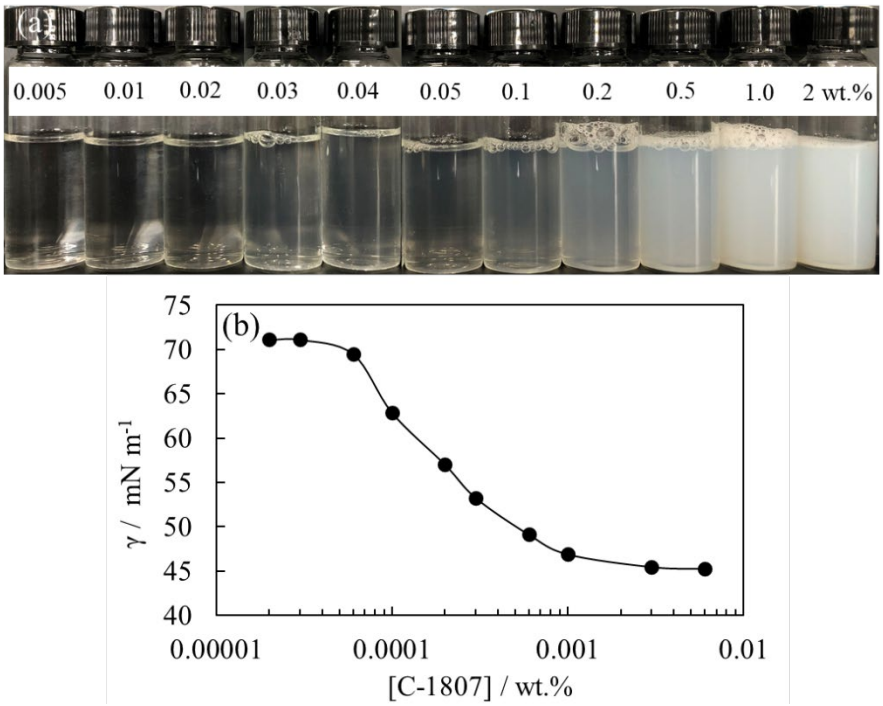

Figure 1. (a) Photos of aqueous dispersions of C-1807 in pure water at different concentrations at 25 ℃ taken 24 h after preparation, (b) air-water surface tension as a function of surfactant concentration at 25 ℃. error bars needed in (b) (We never draw error bars for surface tension carves before since the error bar (±0.2 mN/m) is too small to be seen (shaded by the point)).

Applying the Gibbs adsorption equation to the surface tension-concentration curve, the surface excess (Γ) and the cross-sectional section area (A) of C-1807 molecules at the air-water interface can be calculated:

$$\Gamma = -\left(\frac{1}{2.303RT}\right)\left(\frac{d\gamma}{d\log[C-1807]}\right) \quad (3)$$

$$A = 1/(N_A\Gamma) \quad (4)$$

where R is the gas constant (8.314 J mol^{-1} K^{-1}), T the absolute temperature (293.1 K), γ the surface tension (mN m^{-1}) and N_A is Avogadro's constant (6.023×10^{23} mol^{-1}). Based on the maximum slope obtained from Figure 1(b), the saturated adsorption (Γ_{max}) is calculated to be 1.98×10^{-10} mol/cm^2 corresponding to a minimum molecular area of 0.84 nm^2.

At concentrations above the CAC, the appearance of the mixtures changes gradually from transparent to turbid, suggesting formation of large-sized aggregates in dispersions. This is supported by DLS measurements shown in Figure 2. A bimodal distribution forms at 0.1 wt.% with diameters centred around 200 nm and 1.5 μm. At 1 wt.% however, a multimodal distribution is observed with four populations of aggregate ranging in size from 60 nm to 5 μm.

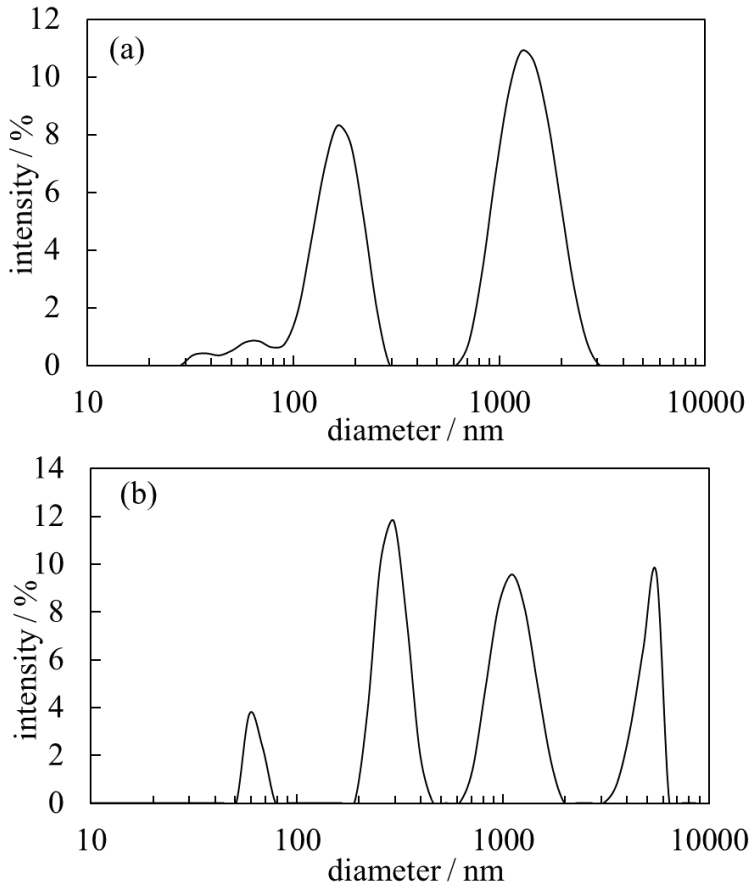

Figure 2. Size distribution of vesicles in aqueous dispersions of C-1807 at (a) 0.1 wt.% and (b) 1.0 wt.%. change size to diameter in both (revised)

Optical microscopy and cryo-TEM images of C-1807 aqueous dispersions are shown in Figure 3(a) and Figure 3(b). Evidence exists that the aggregates are vesicles of different size and most of them are multilamellar. Since the C_{18} hydrocarbon chain has a length around 2 nm, and the smallest diameter of the aggregates observed from DLS is around 30 nm, these aggregates are not micelles but closed vesicles. This is

consistent with results reported by Ishigaml and Machlda[12] who used electron microscopy and fluorescence microscopy to confirm that sucrose fatty acid esters form closed vesicles. The presence of vesicles has also been confirmed in aqueous dispersions of C-1815 (a more hydrophilic sucrose ester) in our previous study.[41]

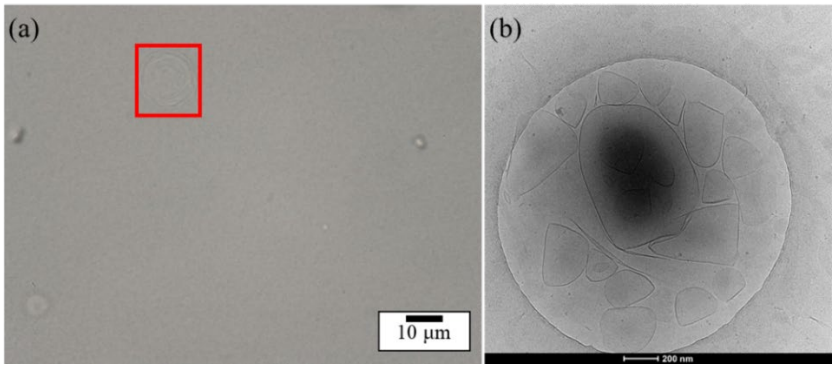

Figure 3. (a) Optical micrograph and (b) cryo-TEM image of C-1807 aqueous dispersions at 2 wt.%. have we any more SEM images? (sorry, we don't have any SEM and cryo-SEM images)

Figure 4(a) shows the variation of steady shear viscosity as a function of shear rate for C-1807 aqueous dispersions at different concentrations at 25 ℃. With increasing shear rate, only the dispersion with 2 wt.% C-1807 shows shear thinning behavior which is attributed to the destruction of large aggregates in dispersion under external forces. In addition, when the concentration of C-1807 is below 1.0 wt.%, the viscosity of C-1807 aqueous solutions is similar with that of water at 25 ℃, suggesting formation of small size vesicles which are less affected by increasing shear rate.

The dynamic rheological behavior of the C-1807 aqueous dispersions at 1 wt.% and 2 wt.% was then investigated by oscillatory shear measurements. As shown in Figure 4(b), a linear viscoelastic region exists for the dispersion at 2 wt.% with increasing strain. However, the dispersion at 1.0 wt.% does not show this region (Figure S1). From Figure 4(c), it is seen that the elastic modulus G' is always greater than the viscous modulus G'' within the investigated frequency range. This indicates that the dispersion at 2 wt.% shows gel-like behavior or viscoelasticity whereas the dispersion

at 1 wt.% is not viscoelastic.

Similar to C-1815,[41] the nonionic aggregates in C-1807 aqueous dispersions have a negative zeta potential around -50 mV at concentration above the CAC as shown in Figure S2 implying that the aggregates are negatively charged. The reason for such a result is not immediately clear, but may be due to adsorption of hydroxyl anions on the surface of the aggregates or to the dissociation of free fatty acid impurity.

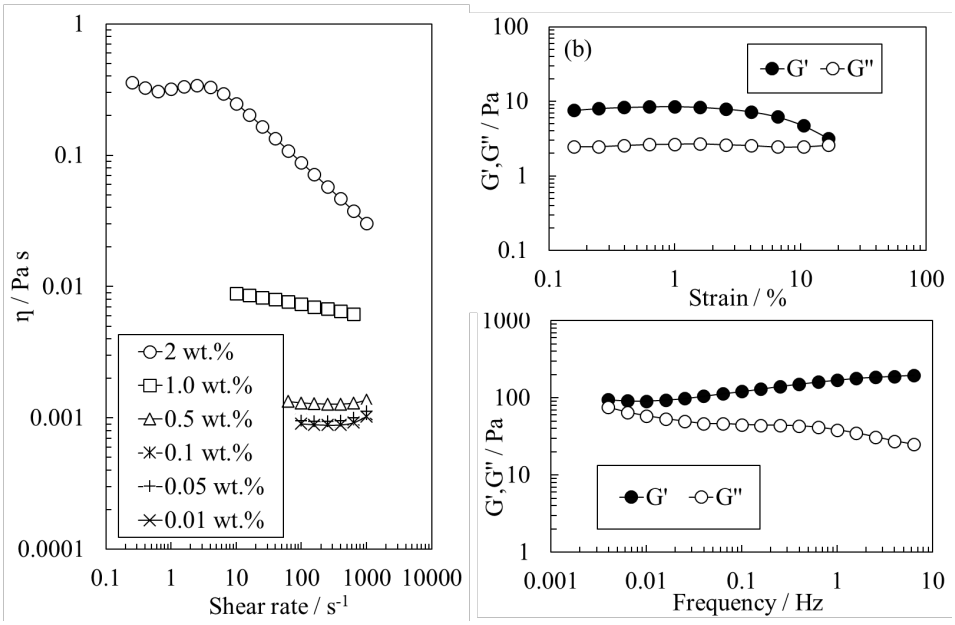

Figure 4. (a) Viscosity of C-1807 aqueous dispersions at different concentrations (as shown) as a function of shear rate at 25 ℃ and (b) variation of storage modulus G'' and loss modulus G' with strain and (c) with shear frequency for C-1807 aqueous dispersion at 2 wt.% at 25 ℃. (a) replace Pa.s by Pa s (revised)

(b) Edible oil-in-water emulsions from C-1807 aqueous dispersions

Emulsions of edible oils (canola oil, olive oil and soybean oil) and aqueous dispersions of C-1807 at different concentrations at an oil:water volume ratio of 1:1 were prepared and characterized. The appearance and optical micrographs of the canola oil-in-water emulsions are shown in Figure 5. It is found that the emulsions formed are O/W type as confirmed by the drop test immediately after preparation. However, at concentrations of C-1807 below 0.1 wt.% (CAC = 5.2×10^{-4} wt.%), the emulsions are

unstable and demulsification occurred completely after 48 h. At concentrations between 0.1 wt.% and 1 wt.%, emulsions are stable within 48 h but demulsification occurred after 2 months. Only at a concentration of 2 wt.% C-1807 was the emulsion stable after 3 months.

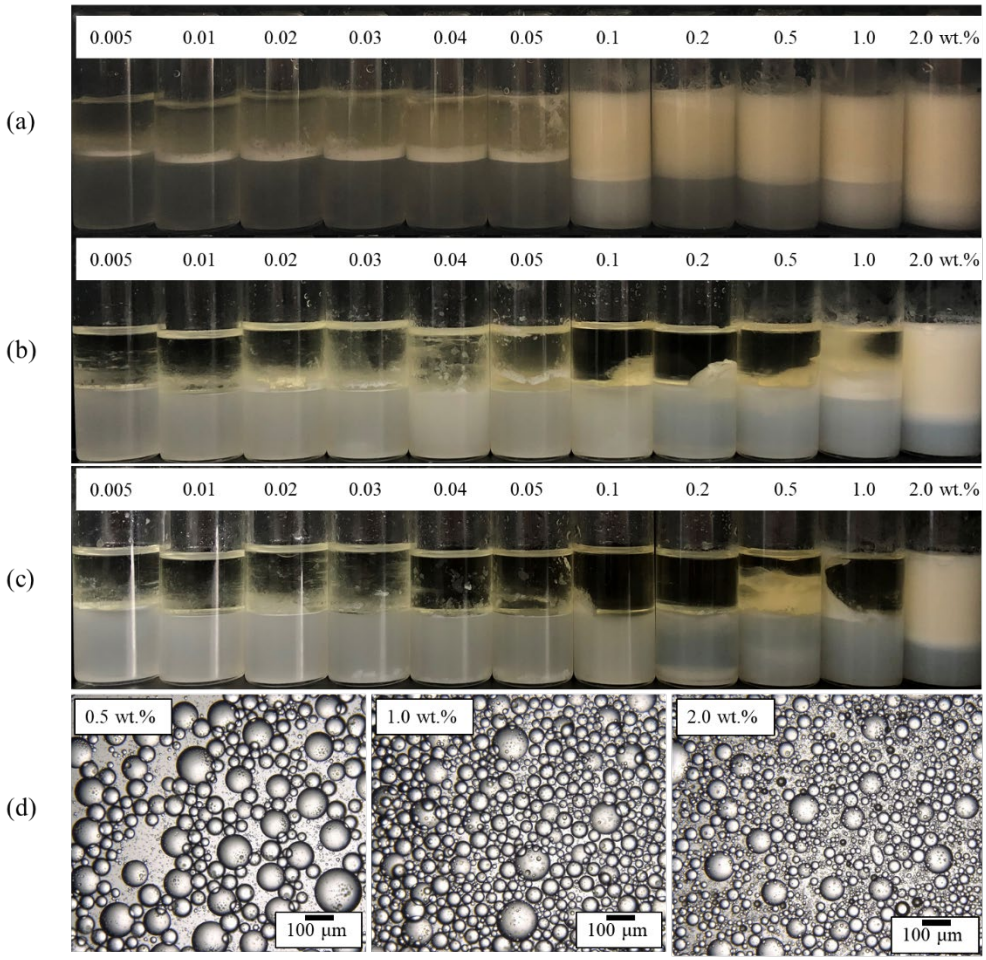

Figure 5. Appearance of canola oil-in-water emulsions with $\phi_o = 0.5$ prepared using C-1807 aqueous dispersions at different concentrations as shown taken (a) 48 h, (b) 2 months and (c) 3 months after preparation at 25 °C, (d) micrographs of selected emulsions taken 24 h after preparation.

The appearance of emulsions formed by olive oil and soybean oil are shown in Figures S3 and S4, respectively. Similarly, the emulsions are all O/W type and they are unstable against creaming and coalescence after 3 months at C-1807 concentrations ≤ 1 wt.%. Even at 2 wt.% C-1807, the emulsion formed are only partially stable after 3

months. The overall stability of the three kinds of edible oil-in-water emulsions to creaming and coalescence after 3 months are summarized in Figure 6 by the parameters f_w and f_o. It is seen that the only difference appears at 2 wt.% C-1807, where the canola oil-in-water emulsion is generally stable, the soybean oil-in-water emulsion is less stable and an olive oil-in-water emulsion is unstable.

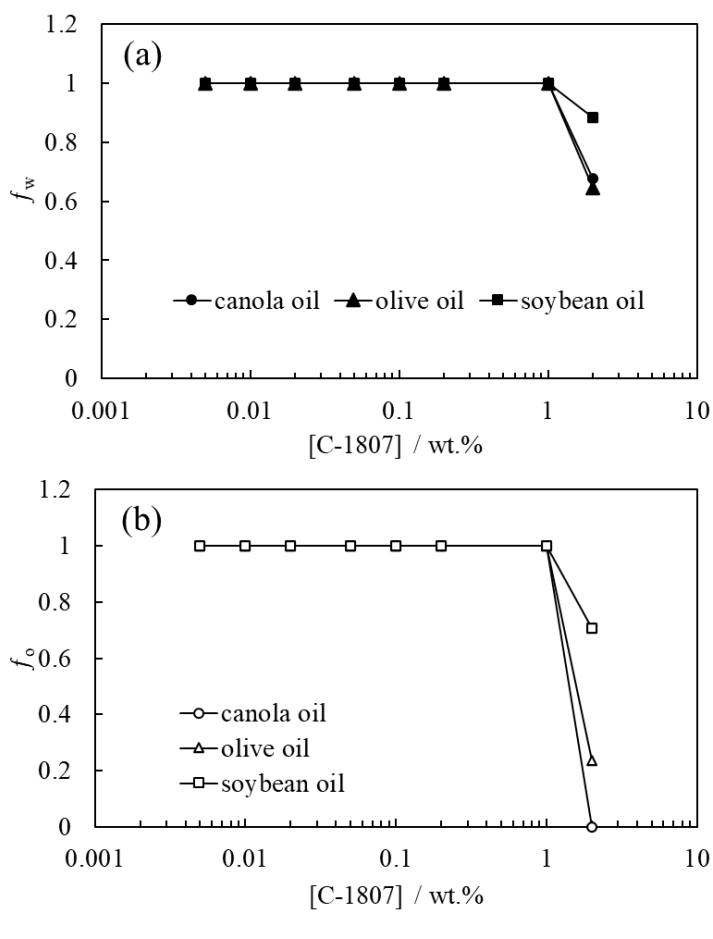

Figure 6. Variation of (a) f_w and (b) f_o with surfactant concentration for three edible oil-in-water emulsions prepared using C-1807 aqueous dispersions after 3 months at 25 °C.

To understand the difference in stabilization between these edible oil-in-water emulsions, the relationship between the structure of the emulsions and macro liquidity is analyzed using the small amplitude oscillation test performed in the linear viscoelastic region (Figure S5). The results are shown in Figure 7(a), where G' and G'' of all emulsions increase slightly with increasing frequency. Moreover, the G' values

are always higher than the corresponding G" at all frequencies ranging from 0.01 to 10 Hz, indicating that these emulsions have a high gel strength.

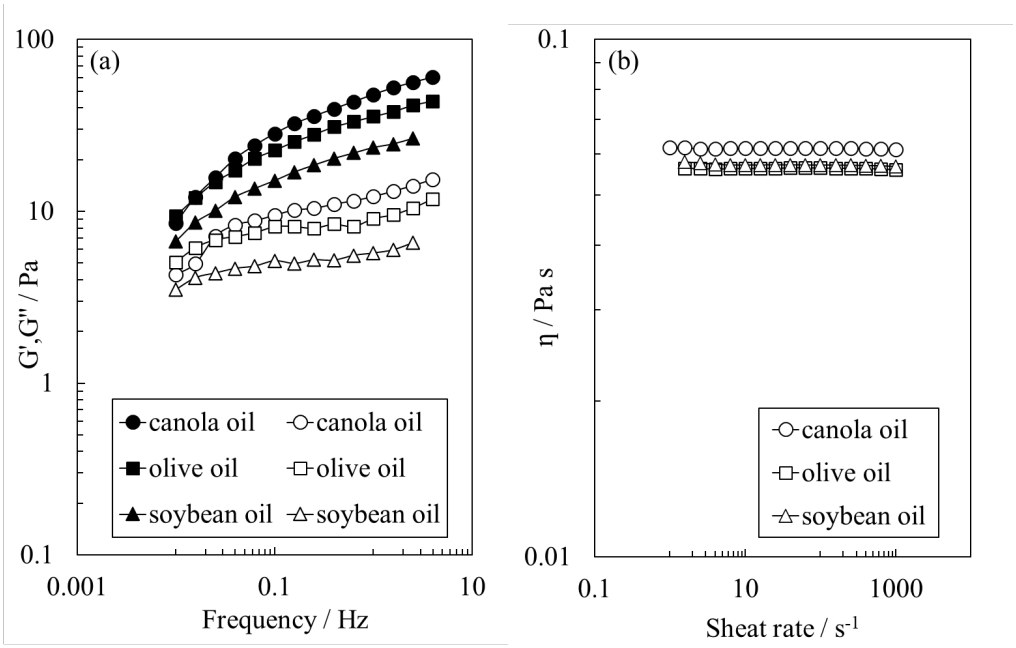

Figure 7. (a) Variation of storage modulus G' (filled points) and loss modulus G'' (open points) with shear frequency for edible oil-in-water emulsions with $\phi_o = 0.5$ prepared using 2 wt.% C-1807 aqueous dispersions measured 24 h after preparation at 25 ℃, (b) viscosity of oils as a function of shear rate at 25 ℃.

Different from conventional nonionic surfactants which can stabilize emulsions when monomeric, here C-1807 is not able to stabilize an O/W emulsion at concentrations lower than CAC. At C-1807 concentrations above the CAC but lower than 0.1 wt.%, vesicles are formed but their amount is not large enough to prevent droplets from flocculation and coalescence. Even at C-1807 concentration between 0.1 wt.% and 1 wt.%, the vesicles formed lead to an improvement in the stability of emulsions but the emulsions lack longtime stability. Only with 2 wt.% C-1807 where a viscoelastic dispersion is formed can edible oil-in-water emulsions become much more stable, especially for canola oil (3 months). Based on DLVO theory,[42] a large concentration of vesicles dispersed in water surrounding oil droplets may weaken the van der Waals attraction between oil droplets. On the other hand, the aqueous dispersion

with 2 wt.% C-1807 shows gel-like behavior, which is beneficial for preventing oil droplets from coalescence. This stabilization mechanism is like what we reported for emulsions stabilized by sucrose ester C-1815, [41] where the mechanism was verified by cryo-SEM images which showed that oil droplets are surrounded by many vesicles. In addition, the vesicles are negatively charged and the repulsion between vesicles in water may be beneficial to form thick lamellae improving emulsion stability.

Nevertheless, emulsions formed by the three different edible oils display different stability at 2 wt.% C-1807. This is not caused by the viscosity of the oils since the three oils have a similar viscosity as shown in Figure 7(b), and neither by the continuous phase or the oil:water ratio since they are same. The only possibility for the difference may come from the composition of the edible oils. We have analysed the composition of the three edible oils using GC/MS (Table S1), and found that although the major components are quite similar the content of each component is different.

(c) HIPEs formed by C-1807 aqueous dispersions

To further understand the stabilization of the emulsions prepared using C-1807 viscoelastic solutions, edible oil-in-water HIPEs with $\phi_o = 0.75$ stabilized by 2 wt.% C-1807 were prepared. Figure 8 shows the appearance and micrographs of the emulsions 24 h after preparation for both canola oil and olive oil (that for soybean oil are shown in Figure S6). It is seen that after 24 h storage at room temperature, emulsions showed no obvious change with neither creaming nor coalescence being observed. The optical micrographs indicate that large and small oil droplets are squeezed together and deformed from spherical. Since there are large amounts of vesicles present in the continuous phase, they tend to constitute walls surrounding the droplets and therefore prevent droplets from coalescence. The stabilization of the three HIPEs can last for at least 1 week. After 45 days the canola oil-in-water HIPE is still stable but partial demulsification (both coalescence and creaming) occurred for the other two HIPEs, and after three months all three HIPEs are no longer stable as shown in Figure S7.

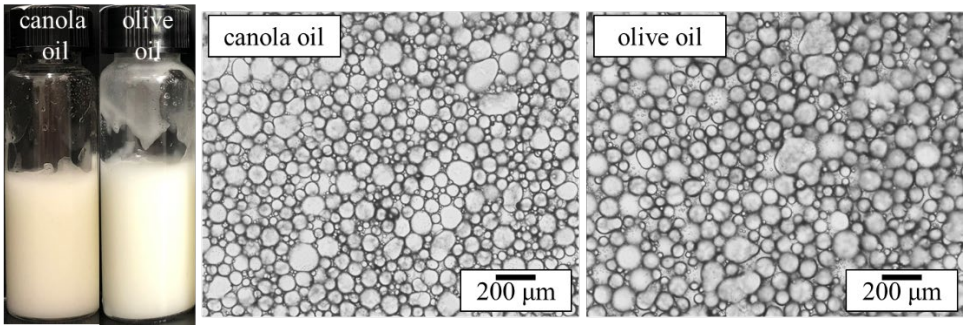

Figure 8. Appearance and optical micrographs of two edible oil-in-water HIPEs with $\phi_o = 0.75$ stabilized by 2 wt.% C-1807 taken 24 h after preparation at 25 °C**.**

In view of applications in the food industry, the cooling-heating and freeze-thaw stability of these edible oil-in-water HIPEs is of interest. We chose 5 °C and -20 °C, the low temperature limits used in a refrigerator and freezer (and freezer?) (Yes, revised), as the low temperature limit and 30 °C as the upper limit to examine the stability of the HIPEs stabilized by C-1807 at 2 wt.% against cooling-heating and freeze-thaw cycles, respectively. For cooling-heating cycles the emulsions prepared at room temperature were first cooled to 5 °C (in a thermostatic bath for 22 h) and then heated to 30 °C for 2 h as one cycle. The appearance of the HIPEs that underwent three cooling-heating cycles are shown in Figure 9. It is seen that for three HIPEs stabilized by viscoelastic solutions, only slight phase separation occurred with increasing number of cycles, and after three cycles only a small portion of water was released. These HIPEs therefore show good stability against cooling-heating cycles.

Similarly, the three HIPEs underwent three freeze-thaw cycles between -20 °C and 30 °C. Unfortunately, after the first freeze-thaw cycle these HIPEs are damaged as phase separation occurred as shown in Figure S8. Oil was released through extensive droplet coalescence and water containing vesicles constitute a viscous gel attached on the glass wall. With increasing freeze-thaw cycle, more oil was released. The HIPEs are thus unstable against freeze-thaw cycles between -20 °C and 30 °C.

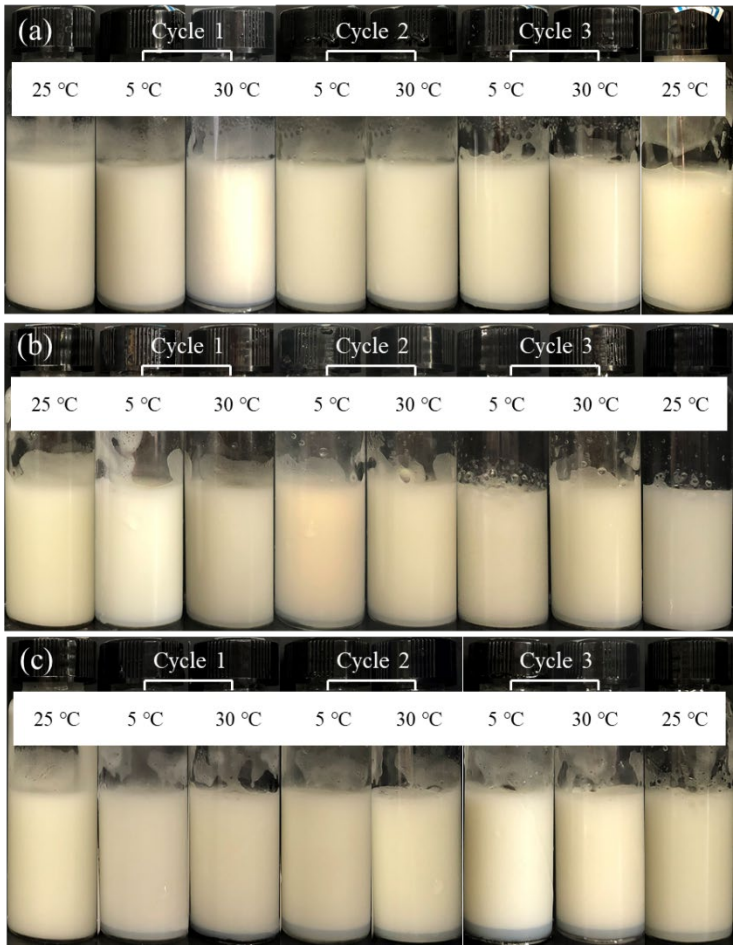

Figure 9. Appearance of edible oil-in-water HIPEs with $\phi_o = 0.75$ stabilized by 2 wt.% C-1807 during three cooling-heating cycles. (a) canola oil, (b) olive oil and (c) soybean oil.

To understand the effect of temperature especially on freezing on the stabilization of HIPEs, DSC analysis was carried out for the three HIPEs stabilized by 2 wt.% C-1807. The samples were cooled from 30 °C to -30 °C and then heated from -30 °C to 30 °C at a rate of ± 5 °C/min as a cycle, and total of three freeze-thaw cycles were carried out for each sample as shown in Figure 10. Similarly, DSC analysis of the three oils was also carried out for comparison, as shown in Figure S9.

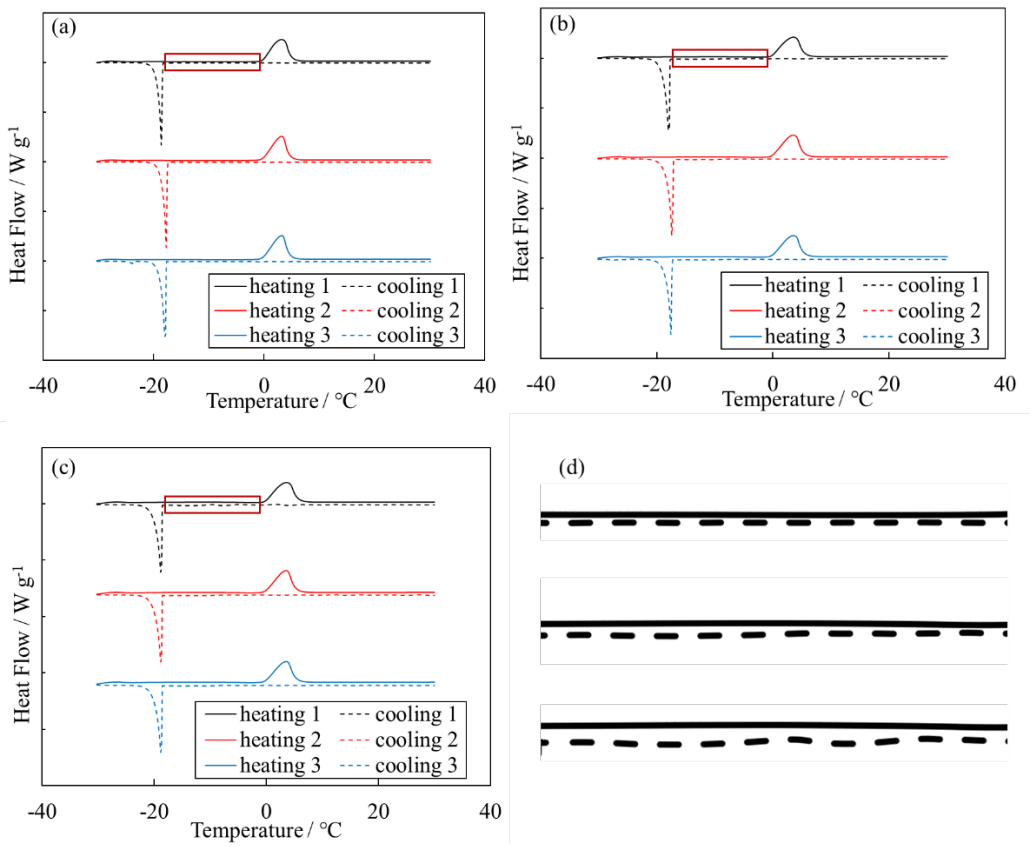

Figure 10. DSC cooling and heating thermograms of three edible oil-in-water HIPEs with $\phi_o = 0.75$ stabilized by 2 wt.% C-1807 at 5 °C/min, from 30 °C to -30 °C to 30 °C. (a) Canola oil, (b) olive oil and (c) soybean oil, (d) (from top) magnified parts shown by the red frames in (a), (b) and (c) respectively.

Form Figure S9, it is seen that the canola oil has a distinct freezing point at around -60 °C far below -20 °C, whereas both soybean oil and olive oil show freezing at a wide temperature range from -50 °C to 0 °C. However, the DSC results for three HIPEs shown in Figure 10 are generally similar. For canola oil, only a sharp exothermic peak appears at around -18 °C, which is identified as water crystallization. In the heating process of the three cycles only one endothermic peak was observed at around 0 °C, which is identified as the melting of water. But for soybean oil and olive oil, a weak exothermic peak begins at -5 °C, as shown magnified in Figure 10(d), which can then be identified as the partial crystallization of soybean oil and olive oil in emulsions. A second sharp exothermic peak appears at around -17 °C, which is identified as water

crystallization. However, the endothermic peak of oil may be very weak. No obvious peak of oil appears during heating and just one endothermic peak of water around 0 °C can be verified.

The above analysis is helpful in understanding the stability of HIPEs stabilized by 2 wt.% C-1807 against cooling-heating and freeze-thaw cycles. In freeze-thaw cycles, ice crystals are formed as the temperature decreases to -20 °C. In addition, partial liquid oil will be crystalized for soybean oil and olive oil. The oil droplets or crystals have opportunity to penetrate through the vesicle lamellae and contact with each other. Upon thawing, oil crystals melted and coalesced into a large droplet causing destabilization of the emulsions. In cooling-heating cycles, however, no ice or oil crystals will be formed as the temperature only reached 5 °C. The oil droplets surrounded by the vesicle lamellae are well separated, and the vesicles in the lamellae and gel-like strength from viscoelastic solutions prevent oil droplets from coalescence.

Conclusions

(1) The nonionic surfactant sucrose stearate C-1807 forms multilamellar vesicles in aqueous solution at concentrations beyond the CAC (5.2×10^{-4} wt.%) and turbid dispersions are formed. At concentration as high as 2 wt.%, the aqueous dispersion becomes viscoelastic and shows gel-like behavior.

(2) Although monomeric C-1807 is not a good emulsifier, edible oil-in-water emulsions with $\phi_o = 0.5$ (for canola oil, olive oil and soybean oil) can be formed by the dispersions where the vesicles can improve the stability of the emulsions. At 2 wt.% C-1807, the canola oil-in-water emulsions with $\phi_o = 0.5$ is stable at room temperature for at least 3 months, and emulsions with olive oil or soybean oil are stable for at least two months. The viscoelastic aqueous phase provides gel-like strength and vesicles dispersed in aqueous lamellae surround oil droplets preventing them from flocculation and coalescence.

(3) High internal phase emulsions (HIPEs) with $\phi_o = 0.75$ can be formed by the viscoelastic aqueous dispersion with 2 wt.% C-1807 and the three edible oils. Although

the HIPEs are not stable against harsh freeze-thaw cycles between -20 °C and 30 °C where ice crystals formed are not beneficial to stability, they are stable against cooling-heating cycles between 5 °C and 30 °C. This characteristic provides a protocol such that sucrose esters like C-1807 with intermediate HLB numbers can be used as a food-grade emulsifier in food emulsion products.

Acknowledgements

The authors thank the China Scholarship Council for funding XH and the University of Hull for hosting her stay.

References

1. S. Jung, H. Choi, Fruit Quality and Antioxidant Activities of Yellow-Skinned Apple Cultivars Coated with Natural Sucrose Monoesters, *Sustainability* **13** (2021) 2423.
2. Arpathsra Sangnarka, Athapol Noomhorm, Effect of dietary fiber from sugarcane bagasse and sucrose ester on dough and bread properties, *Lebensm.-Wiss. u.-Technol*. **37** (2004) 697–704.
3. F.Ahsan, J. J. Arnold, E. Meezan, D. J. Pillion, Sucrose cocoate, a component of cosmetic preparations, enhances nasal and ocular peptide absorption, Sucrose cocoate, a component of cosmetic preparations, enhances nasal and ocular peptide absorption, *Int. J. Pharm*. **251** (2003) 195-203.
4. K. Valdés, M. J. Morilla, E. Romero, J. Chávez, Physicochemical characterization and cytotoxic studies of nonionic surfactant vesicles using sucrose esters as oral delivery systems, *Colloids Surf. B* **117** (2014) 1–6.
5. V. M. Sadtler, M. Guely, P. Marchal, L. Choplin, Shear-induced phase transitions in sucrose ester surfactant, *J. Colloid Interface Sci*. **270** (2004) 270–275.
6. J. J. Rao, D. J. McClements, Food-grade microemulsions, nanoemulsions and emulsions: Fabrication from sucrose monopalmitate & lemon oil, *Food Hydrocolloids* **25** (2011) 1413-1423.
7. M. Ludwig, R. Geisler, S. Prévost, R. V. Klitzing, Shape and Structure Formation of Mixed Nonionic–Anionic Surfactant Micelles, *Molecules* **26** (2021) 4136.
8. T. M. McCoy, J. B. Marlow, A. J. Armstrong, A. J. Clulow, C. J. Garvey, M. Manohar, T. A. Darwish, B. J. Boyd, A. F. Routh, R. F. Tabor, Spontaneous Self-Assembly of Thermoresponsive Vesicles Using a Zwitterionic and an Anionic Surfactant, *Biomacromolecules* **21** (2020) 4569−4576.
9. C. P. Baryiames, M. Teel, C. R. Baiz, Interfacial H-Bond Dynamics in Reverse Micelles: The Role of Surfactant Heterogeneity, *Langmuir* 35 (2019) 11463−11470.
10. H. G. Li, X. Xin, T. Kalwarczyk, R. Hołyst, J. F Chen, J. C. Hao, Structural evolution of reverse vesicles from a salt-free catanionic surfactant system in toluene, *Colloids Surf. A* **436** (2013) 49–56.

11. M. Ramanathan, L. K. Shrestha, T. Mori, Q. M. Ji, J. P. Hillbc, K. Ariga, Amphiphile nanoarchitectonics: from basic physical chemistry to advanced applications, *Phys. Chem. Chem. Phys.* **15** (2013) 10580-10611.
12. Y. Ishigaml, H. Machlda, Vesicles From Sucrose Fatty Acid Esters, *J. Am. Oil Chem. Soc.* **66** (1989) 599-603.
13. H. Mollee, J. D. Vrind, T. D. Vringer, Stable Reversed Vesicles in Oil: Characterization Studies and Encapsulation of Model Compounds, *J. Pharm. Sci*. **89** (2000) 930-939.
14. C. Marianecci, D. Paolino, C. Celia, M. Fresta, M. Carafa, F. Alhaique, Non-ionic surfactant vesicles in pulmonary glucocorticoid delivery: Characterization and interaction with human lung fibroblasts, *J. Contr. Release* **147** (2010) 127–135.
15. R. Cortesi, E. Esposito, F. Corradini, E. Sivieri, M. Drechsler, A. Rossi, A. Scatturin, E. Menegatti, Non-phospholipid vesicles as carriers for peptides and proteins: Production, characterization and stability studies, *Int. J. Pharm*. **339** (2007) 52–60.
16. L. D. Marzioa, C. Marianecci, M. Petronea, F. Rinaldi, M. Carafa, Novel pH-sensitive non-ionic surfactant vesicles: comparison between Tween 21 and Tween 20, *Colloids Surf. B* **82** (2011) 18–24.
17. R. Abdel-Rahem, H. Hoffmann, The distinction of viscoelastic phases from entangled wormlike micelles and of densely packed multilamellar vesicles on the basis of rheological measurements, *Rheol. Acta*. **45** (2006) 781–792.
18. Y. Takahashi, Y. Yamamoto, S. Hata, Y. Kondo, Unusual viscoelasticity behaviour in aqueous solutions containing a photoresponsive amphiphile, *J. Colloid Interface Sci*. **407** (2013) 370–374.
19. Y. M. Hu, J. Han, L. L. Ge, R. Guo, Viscoelastic wormlike micelles formed by ionic liquid-type surfactant [C16imC8]Br towards template-assisted synthesis of CdS quantum dots, *Soft Matter* **14** (2018) 789-796.
20. A. V. Shibaeva, D. Yu. Mityuka, D. A. Muravleva, O. E. Philippova, Viscoelastic Solutions of Wormlike Micelles of a Cationic Surfactant and a Stiff-Chain Anionic Polyelectrolyte, *Polym. Sci. Ser. A+* **61** (2019) 765–772.

21. L. Garcia-Rio, J. C. Mejuto, M. Perez-Lorenzo, A. Rodriguez-Alvarez, P. Rodriguez-Dafonte, Influence of Anionic Surfactants on the Electric Percolation of AOT/Isooctane/Water Microemulsions, *Langmuir* **21** (2005) 6259-6264.
22. B. L. Cushing, V. L. Kolesnichenko, C. J. O'Connor, Recent Advances in the Liquid-Phase Syntheses of Inorganic Nanoparticles, *Chem. Rev*. **104** (2004) 3893−3946.
23. D. Wang, G. C. Wei, R. H. Dong, J. C. Hao, Multiresponsive Viscoelastic Vesicle Gels of Nonionic C12EO4 and Anionic AzoNa, *Chem. Eur. J*. **19** (2013) 8253-8260.
24. N. R. Agrawal, M. Omarova, F. Burni, V. T. John, S. R. Raghavan, Spontaneous Formation of Stable Vesicles and Vesicle Gels in Polar Organic Solvents, *Langmuir* **37** (2021) 7955−7965.
25. R. Cao, D. Kumar, A. D. Dinsmore, Vesicle-Based Gel via Polyelectrolyte-Induced Adhesion: Structure, Rheology, and Response, *Langmuir* **37** (2021) 1714−1724.
26. N. R. Cameron, D. C. Sherrington, High internal phase emulsions (HIPEs) - structure, properties and use in polymer preparation. *Adv. Polym. Sci*. **126** (1996) 163–214.
27. L. L. Xu, L. P. Gu, Y. J. Su, C. H. Chang, S. J. Dong, X. H. Tang, Y. J. Yang, J. H. Li, Formation of egg yolk-modified starch complex and its stabilization effect on high internal phase emulsions, *Carbohyd. Polym*. **247** (2020) 116726.
28. W. Liu, H. X. Gao, D. J. McClements, L. Zhou, J. Wu, L. Q. Zou, Stability, rheology, and β-carotene bioaccessibility of high internal phase emulsion gels, *Food Hydrocolloid*s **88** (2019) 210–217.
29. W. Li, Y. Q. Nian, Y. C. Huang, X. X. Zeng, Q. Chen, B. Hu, High loading contents, distribution and stability of β-carotene encapsulated in high internal phase emulsions, *Food Hydrocolloids* **96** (2019) 300–309.
30. H. X. Gao, L. Ma, C. Cheng, J. P. Liu, R. H. Liang, L. Q. Zou, W. Liu, D. J. McClements, Review of recent advances in the preparation, properties, and applications of high internal phase emulsions, *Trends Food Sci. Technol*. **112** (2021) 36–49.

31. J. L. Su, X. Q. Wang, W. Li, L. G. Chen, X. X. Zeng, Q. R. Huang, B. Hu, Enhancing the Viability of Lactobacillus plantarum as Probiotics through Encapsulation with High Internal Phase Emulsions Stabilized with Whey Protein Isolate Microgels, *J. Agric. Food Chem*. **66** (2018) 12335−12343.
32. H. Tan, G. Q. Sun, W. Lin, C. D. Mu, T. Ngai, Gelatin Particle-Stabilized High Internal Phase Emulsions as Nutraceutical Containers, *ACS Appl. Mater. Interfaces* **6** (2014) 13977−13984.
33. J. Y. Miao, N. Xu, C. Cheng, L. Q. Zou, J. Chen, Y. Wang, R. H. Liang, D. J. McClements, W. Liu, Fabrication of polysaccharide-based high internal phase emulsion gels: Enhancement of curcumin stability and bioaccessibility, *Food Hydrocolloid*s **117** (2021) 106679.
34. F. Z. Zhou, T. Zeng, S. W. Yin, C. H. Tang, D. B. Yuan, X. Q. Yang, Development of antioxidant gliadin particle stabilized Pickering high internal phase emulsions (HIPEs) as oral delivery systems and the in vitro digestion fate, *Food Funct*. **9** (2018) 959-970.
35. X. N. Huang, F. Z. Zhou, T. Yang, S. W. Yina, C. H. Tang, X. Q. Yang, Fabrication and characterization of Pickering High Internal Phase Emulsions (HIPEs) stabilized by chitosan-caseinophosphopeptides nanocomplexes as oral delivery vehicles, *Food Hydrocolloid*s **93** (2019) 34–45.
36. B. Jiao, A. Shi, Q. Wang, B. P. Binks, High-Internal-Phase Pickering Emulsions Stabilized Solely by PeanutProtein-Isolate Microgel Particles with Multiple Potential Applications, *Angew. Chem. Int. Ed*. **57** (2018) 9274 –9278.
37. M. Paljevac, P. Krajnc, Hierarchically porous poly(glycidyl methacrylate) through hard sphere and high internal phase emulsion templating, *Polymer* **209** (2020) 123064.
38. G. Q. Sun, Z. F. Li, T. Ngai, Inversion of particle-stabilized emulsions to form high-internal-phase emulsions, *Angew. Chem. Int. Ed*. **49** (2010) 2163-2166.
39. C. Calahorro, J. Mufioz, M. Berjano, A. Guerrero, C. GaUegos, Flow behavior of sucrose stearate/water systems, *J. Am. Oil Chem. Soc*. **69** (1992) 660-666.

40. G. Garofalakis, B. S. Murray, D. B. Sarney, Surface activity and critical aggregation concentration of pure sugar esters with different sugar headgroups, *J. Colloid Interface Sci*. **229** (2000) 391-398.
41. X. Hu, B. P. Binks, Z. G. Cui, High internal phase emulsions stabilized by adsorbed sucrose stearate molecules and dispersed vesicles, *Food Hydrocolloids* **121** (2021) 107002.
42. T. Missana, A. Adell, On the applicability of DLVO theory to the prediction of clay colloids stability, *J. Colloid Interface Sci*. **230** (2000) 150-157.

TOC

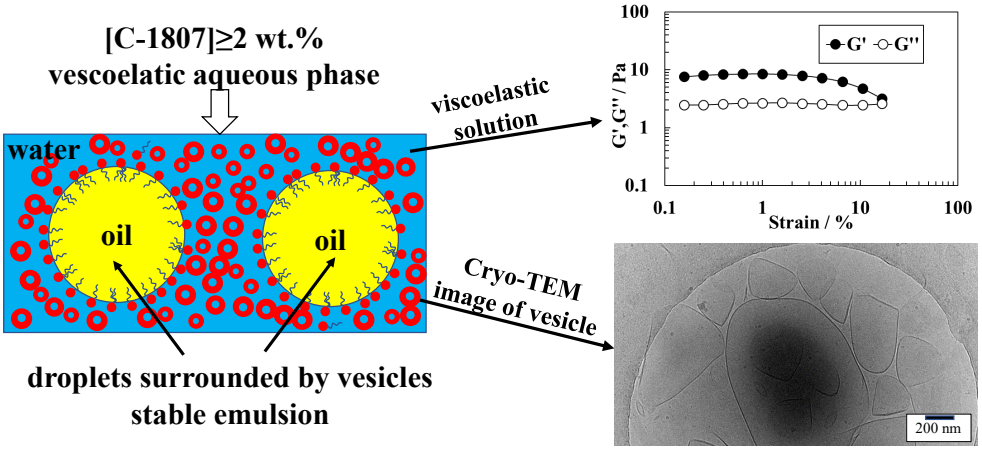

all text should be bold (revised)